

Geochemistry of Amphibolites in Akom II, Nyong Series, North Western Border of the Congo Craton, South Cameroon

Beyanu Anehumbu Aye ^{1*}, Primus Azinwi Tamfuh ^{1,2}, Enerst Tata¹

¹ Department of Mining and Mineral Engineering, National Higher Polytechnic Institute (NAHPI), The University of Bamenda, P.O. Box 39, Bambili, Cameroon

² Department of Soil Science, Faculty of Agronomy and agricultural Sciences, University of Dschang, P. O. Box 222 Dschang, Cameroon

*Corresponding author E-mail: ayebeyanu@yahoo.fr

Abstract

The garnet amphibolites, from the Akom II area in the Archaean Congo Craton, were examined to determine the geochemical affinity and tectonic environment. The study uses mineral assemblages and whole-rock geochemistry to identify the geochemical affinity and tectonic setting of the amphibolites associated with monzogabbro and pyroxenites. The studied rocks of Akom II are garnet amphibolites. Mineralogically, the rocks contain hornblende + plagioclase + garnet ± quartz ± epidote ± apatite ± opaque, indicating that they could have been formed from a basic igneous protolith. The geochemical signature indicates that the rocks are tholeiitic in nature. They are similar to the metamorphosed equivalents of ocean island basalts (OIB), with characteristics typical of Volcanic Arc-Basalt (VAB). The geotectonic diagrams confirm the tholeiitic nature of these amphibolites. High field strength elements ratios (Nb/Ta) range from 14-16, which corresponds to Volcanic Arc Basalt (VAB). The primitive mantle normalized patterns of these rocks show negative anomalies in Ta and Ti suggesting a geotectonic signature characteristic of a subduction zone, consequently suggesting the existence of a suture zone in the study area.

Keywords: Amphibolites; Congo Craton; Geochemistry; Geotectonic Environment; South Cameroon.

1. Introduction

Amphibolites, amphibolitic gneisses, and calcic gneisses usually form remnants of greenstone and metamorphic belts (Wang et al. 2008, Kakar et al. 2014, Tushar M Meshram et al. 2017). They occur in the most diversified geotectonic environments of the planet from the Archaean to the Phanerozoic (Bicalho et al. 2019). Penaye et al. 1989 described the amphibolites as Paleoproterozoic; Munyanyiwa et al. 1997 attested that the amphibolite facies of the Zambezi belt were Neoproterozoic. According to M.T. Gómez-Pugnaire et al. 2003, the amphibolites from the Southwestern Iberian Massif were Upper Precambrian and Lower Palaeozoic (Ordovician). While Fotzing et al. 2019, showed that the amphibolites of the Central African Fold Belt evolved during the Proterozoic. The investigated amphibolites present diverse geochemical affinities: Some are of predominantly tholeiitic composition (Szczepanski, and Oberc-Dziedzic 1998, Bicalho et al. 2019). Others originated from an intra-continental back-arc setting also showing oceanic affinities. Meanwhile some amphibolites were calc-alkaline in nature with characteristics of arc-type basalts (M.T. Gómez-Pugnaire et al. 2003, Fozing et al. 2019). Several studies were conducted within the Nyong unit of the Archaean Congo craton (Ebah Abeng et al. 2012, Aye et al. 2017) yet no one settles the geochemical affinity and tectonic environment of the rocks. The chemical composition of the major and trace elements in rocks, combined with the field petrotectonic association, allows for the identification of the geochemical behaviour and the possible geotectonic environments of their formation (Maniesi & Oliveira 2000, Xu et al. 2008, Faleiros et al. 2011). This paper investigates the petrography, mineralogy and geochemistry of amphibolites of the Nyong unit. It is intended to identify the geochemical affinity and tectonic environment of the generation of amphibolites in this area.

2. Regional geological setting

The Akom II area is situated in the Nyong unit. It forms part of the north western border of the Congo Craton. The northwestern margin of the Archaean Congo craton in Southern Cameroon is commonly known as the Ntem complex (Nédélec et al. 1990; Shang et al. 2010). The Ntem complex is bordered in the north by the Yaounde Group of the Pan-African orogenic belt in Central Africa (Nzenti et al. 1988; Toteu et al. 2006), (Fig.1). The two entities are delimited by a major thrust fault of Pan-African age (600 Ma). The Ntem complex comprises of Palaeoarchaean to Mesoarchaean and Late Archaean charnockites, Mesoarchaean greenstone formations, Late Archaean TTG basement, dolerite dykes and high-K granites (Shang et al. 2010). Based on the lithology and ages, this complex is divided from East to West in to three tectonic units (Tchameni et al. 2004, Aye et al. 2017): Ntem, Nyong, and Ayina units (Fig. 1).



The Ntem unit is Archaean in age and is distinguished: (i) Iron formations associated to amphibolites; (ii) The green stone complexes (Maurizot et al. 1986) (Fig.1). The Ayina unit is Paleoproterozoic in age. It contains rocks which are grouped under the foliated series, and the rocks of this unit are similar to those of Ntem unit (Maurizot et al. 1986, Toteu et al. 1994). The amphibolites of Akom II area belong to the Nyong unit (Penaye et al. 2004). The Nyong unit is made up of a foliated series and a greenstone belt: (i) the foliated series include gneisses, amphibolites, amphibole gneisses and calcic gneisses which outcrop enormously in the studied area (Fig. 1). This series is intercepted locally by mafic or ultramafic veins represented by gabbros, dolerites, and peridotites; (ii) the green stone belt is comprised of ferriferous quartzites, garnet amphibolites, pyroxenites, granitiferous gneisses, leucocratic to mesocratic gneisses. The above rocks make up the green stone belt of the Nyong unit (Toteu et al. 1994; Fig. 1).

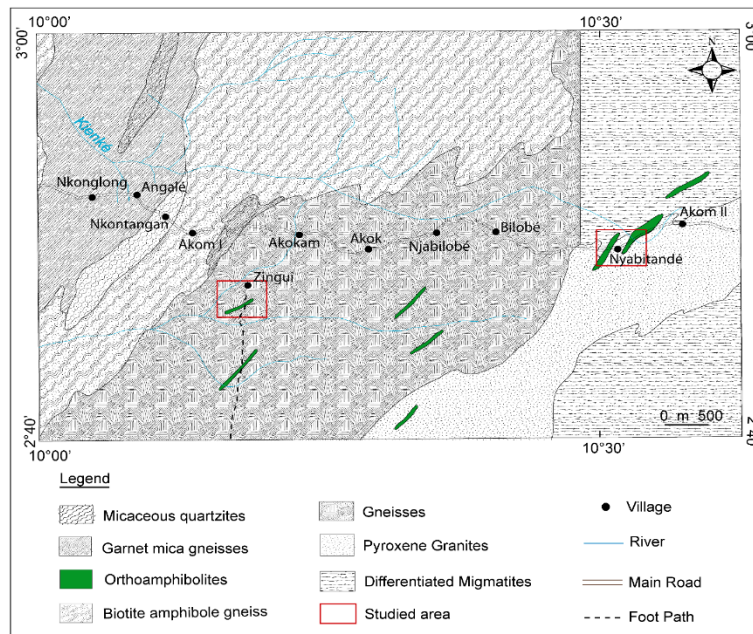


Fig. 1: Geologic Map of Nyabitande and Zingui Areas (Champetier De Ribes and Aubague, 1956).

3. Sampling and analytical methods

A total of thirteen samples were collected and analyzed (Table 1). Eleven of these samples were visibly amphibolites. The other two (pyroxenite and monzogabbro) constitute the country rocks. The above rocks were collected from Nyabitande and Zingui areas.

Samples were crushed in the Department of Earth Sciences (University of Yaoundé 1, Cameroon). The mineralogical analyses were done at Geoscience Laboratories. The analytical instrument is PAN Analytical X'PERT PRO diffractometer equipped with a monochromator using a Co K α radiation of 1.7854Å over a range of 2.5° to 35° 2 θ and a step size of 0.05° 2 θ /min at 40 kV and 45 mA. Chromium and Ni contents were determined by ICP-MS after aqua regia digestion at Geoscience Laboratories (Sudbury, Canada). Samples analyzed for a suite of major and trace elements at the Geoscience Laboratories were crushed using a jaw crusher with steel plates and pulverized in a ball mill made of 99.8% Al₂O₃. A two-step loss on ignition (LOI) determination was carried out. Powders were first heated at 105 °C in the presence of nitrogen to drive off absorbed H₂O and then ignited at 1000 °C in the presence of oxygen to eliminate the remaining volatile components and oxidize Fe. Major element concentrations were determined by X-ray Fluorescence after sample ignition. Sample powders were fused using lithium tetraborate flux before analysis with a Rigaku RIX-3000 wavelength-dispersive X-ray Fluorescence spectrometer. Rock powders were digested by acid attack in closed beakers for Inductively Coupled Plasma-Mass Spectrometry (ICP-MS) analysis for lithophile trace element concentrations. Powders were treated in a mixture of HCl and HClO₄ acids at 120 °C in sealed Teflon containers for one week, and then rinsed from their containers with dilute HNO₃ and dried. The residue was again dissolved in an acid mixture (HCl and HClO₄) and evaporated to dryness a second time, before being dissolved again in a mixture of three acids (HNO₃, HCl, and HF) at 100 °C. Sample solutions were analyzed using Perkin Elmer Elan 9000 ICP-MS instrument.

4. Results

4.1. Petrography and mineralogy

The garnet amphibolites appear frequently under the thick vegetation cover of Nyabitande, in the form of diverse rounded and spherical blocks of different dimension (Fig. 2a) They are melanocratic and medium to coarse grained (Fig. 2b). They are made up of amphibole (green hornblende ~55%), plagioclase (~18%), garnet (~15%), biotite (~5%) and quartz (~5%) (Fig. 2c and d). Accessorily, they consist of Zircon, apatite, sphene and opaque minerals (Fig. 2-f). The crystal size of amphibole occurs as microblast and phenoblast which can attain 2 mm (Fig. 2c and d). Plagioclase crystals present xenoblastic forms of varied sizes (0.04 - 1 mm; Fig. 2c and d). Plagioclase crystals are slightly weathered (Fig. 2f). Garnet grains are porphyroblastic, globular with skeletal to sub rounded crystals (Fig. 2c). Meanwhile, plagioclase and opaque minerals occur mainly in the interstices of the amphibole grains (Fig. 2d and e). Quartz occurs as microblast ranging from 0.06 to 0.3 mm in size and is usually xenoblastic. Meanwhile, the opaque minerals occur as xenoblasts nodules of variable sizes. The detailed observations under metallographic microscope show that the opaque minerals are made up of chalcopyrite and pyrite. Observed diffractograms from X-ray diffractions show that the rocks have primary minerals like amphibole, feldspar, pyroxene, garnet and quartz (Fig.3).

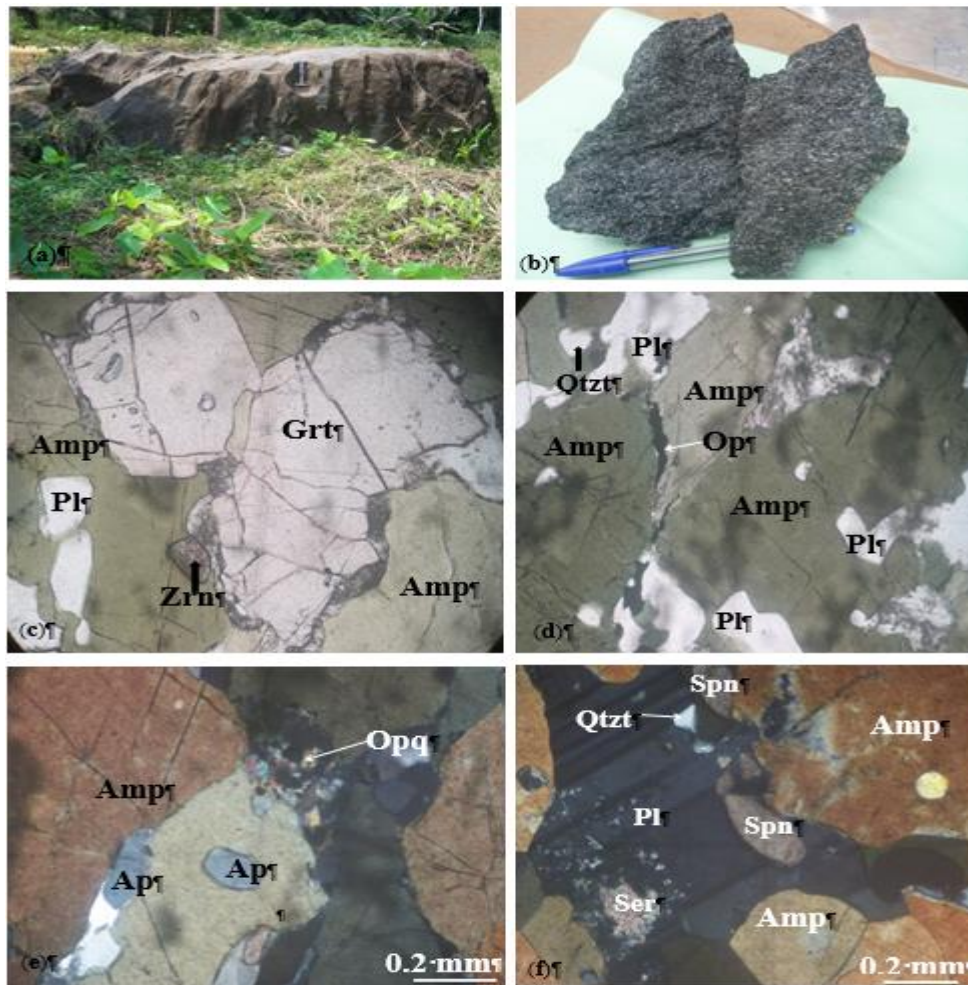


Fig. 2: Macroscopic Organization of Garnet Amphibolites Photographs and Photomicrographs of the Selected Samples: (A -B) Photographs of The Garnet Amphibolite Blocks; (C-F) Photomicrographs of the Garnet Amphibolites (Am = Amphibole; Ap = Apatite; Op = Opaque Minerals; Pl = Plagioclase; Grt = Garnet; Ser: Sericite; Sp: Spinel); Zrn= Zircon

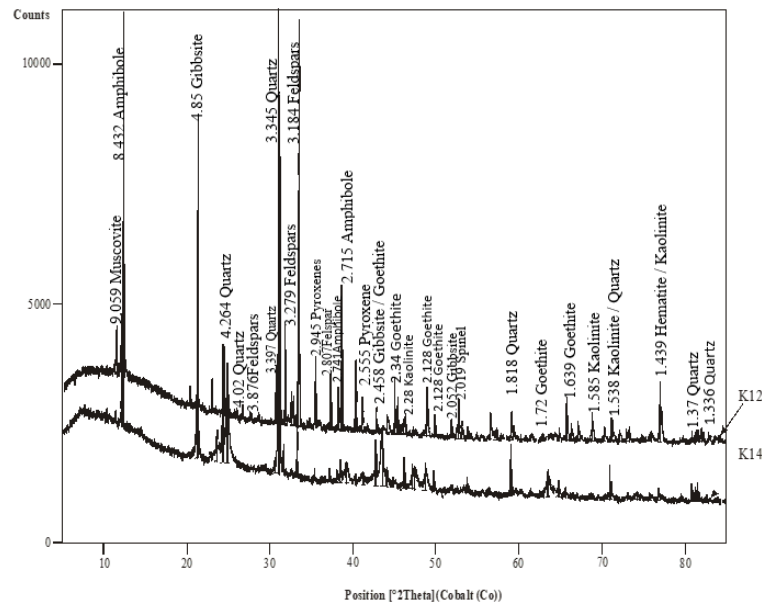


Fig. 3: X-Ray Patterns of Some Slightly Weathered Amphibolite Samples.

4.2. Geochemistry of amphibolites and country rocks

4.2.1. Geochemistry of amphibolites

The SiO₂ content of garnet amphibolites is within the range of a normal mafic rock (44–49 wt.%). Garnet amphibolites are characterized by moderate contents in Al₂O₃ (13–17 wt.%), Fe₂O₃ (14–20 (8 wt.%), and CaO –10 wt.%.)

Amphibolites have very low alkali contents K₂O (0.21 wt. % and Na₂O (0.25 wt. %). They are poor in other oxides like TiO₂, P₂O₅, and MnO. Contents of other major elements are less than or equal to 1 wt. % (Table 1). Amphibolites from Nyabiande have higher contents of

silica than those from Zingui. (Table 1). The LOI values range from 0.3 to 1.0 % for amphibolites. The lower values of LOI in garnet amphibolites suggest less alteration (Kakar et al. 2014).

Geochemical variations reveal positive correlations for Fe_2O_3 with MnO and P_2O_5 . Amphibolites have high contents of Cr, V, Ni, Cu, Zn and Sr. These contents attain several hundreds of ppm. Co, Sc, Zr and Y have contents which attain tens of ppm. The contents of other trace elements are rather low. The amphibolites from Zingui have higher Cr, Sr and Ba contents compared to those of Nyabitande. Contents of rare earth elements are generally low in amphibolites. The sum of REE varies between 36 and 272 ppm. Despite the low contents, the rocks are marked by enrichment in light rare earth elements (LREE; 25-226.4 ppm) than the heavy rare earth elements (HREE; 11-46.53 ppm). The rock/chondrite normalized patterns (McDonough and Sun 1995; Fig. 4) shows significant enrichment in LREE. This is typical of ocean island basalt (OIB).

These normalized patterns reveal negative Eu anomalies and low degree of fractionation. This is confirmed by an enrichment (> 10) of REE within amphibolites. Xenoliths of amphibolites collected from the country rocks of Zingui are particularly rich in REE (Fig. 4b).

Table 1: Major Element Contents (in Wt. %) for Rocks of Akom II.

	Zingui							Kolasseng I									
	1	2	1	1	1	1	1	NK1	NK2	NK3	NK4	NK5	NK7	FN3	AY1	AY2	AY3
SiO ₂	0.04	47.11	44.79	68.1	48.68	47.81	49.30	48.39	49.95	47.75	49.20	48.49	48.76	49.00	49.29	48.84	56.56
Al ₂ O ₃	0.02	15.41	11.04	15.3	12.81	13.37	12.95	13.94	14.36	13.95	14.99	13.62	15.08	12.18	14.02	13.34	21.04
Fe ₂ O ₃	0.01	11.48	18.83	3.2	13.35	14.56	17.09	14.72	12.31	15.20	14.83	14.65	13.63	17.40	14.00	14.85	5.45
CaO	0.01	11.47	11.85	3.7	11.08	11.14	8.91	10.42	11.56	10.51	10.94	10.87	11.11	10.57	10.79	10.81	7.37
MgO	0.01	9.36	7.80	1.1	8.13	7.17	5.07	6.50	7.75	6.48	5.56	6.86	6.86	6.62	6.73	6.72	1.27
Na ₂ O	0.02	2.10	1.27	4.7	2.47	1.90	2.15	1.99	1.97	2.03	1.85	2.64	0.25	1.62	2.58	2.51	6.93
K ₂ O	0.01	0.33	1.15	1.0	0.50	0.51	0.68	0.34	0.28	0.36	0.24	0.26	0.21	0.27	0.40	0.38	0.23
MnO	0.01	0.13	0.28	0.1	0.19	0.30	0.25	0.21	0.20	0.26	0.23	0.21	0.22	0.32	0.15	0.13	0.06
P ₂ O ₅	0.01	0.07	0.72	0.1	0.09	0.09	0.18	0.17	0.07	0.16	0.09	0.16	0.09	0.20	0.15	0.16	0.18
TiO ₂	0.01	0.73	1.03	0.3	1.25	1.40	1.64	1.47	1.08	1.45	1.14	1.45	1.19	1.74	1.31	1.92	0.48
LOI	0.05	0.80	1.03	1.2	0.72	0.85	0.95	0.62	0.61	0.69	0.65	0.27	0.64	0.49	0.74	0.62	0.62
Total		98.97	99.80	98.6	99.28	99.10	99.18	98.77	100.14	98.84	99.71	99.47	100.02	100.4	100.16	100.41	100.20

d.l.: detection limit; LOI: Loss on Ignition 1: Amphibolites; 2: Monzogabbro; 3: Pyroxenite

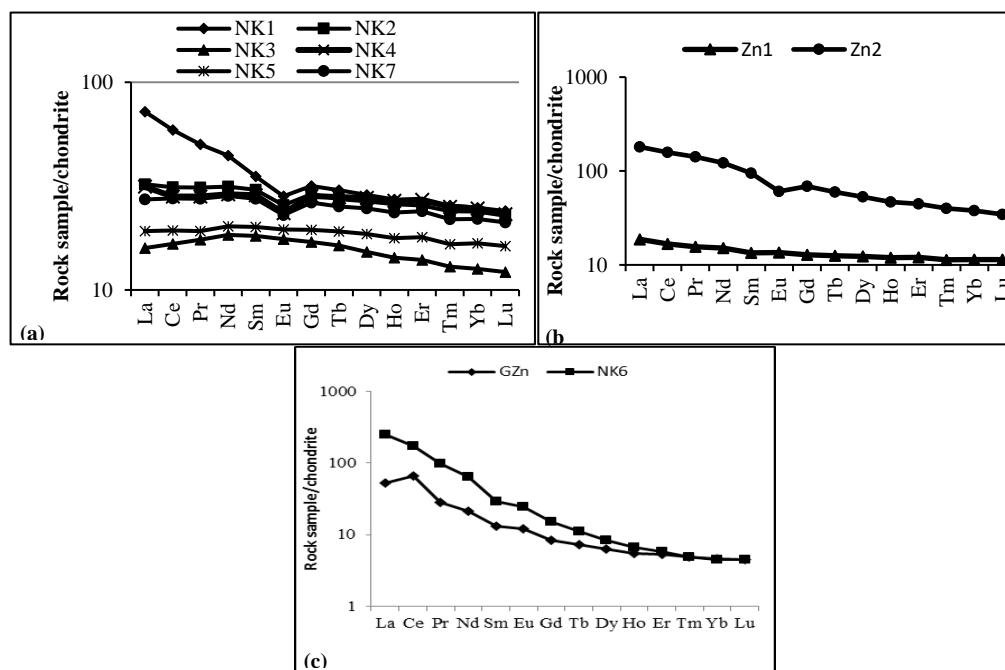


Fig. 4: Chondrites Normalized REE Patterns for Amphibolites. Chondrite Data from McDonough and Sun (1995). A), Nyabitande Samples, B) Zingui Samples and C) Country Rocks.

4.2.2. Geochemistry of country rocks

The major elements of the monzogabbro are characterized by high SiO₂ (68.0 %) and Al₂O₃ contents (15.3 %). They have comparatively lower concentrations of Fe₂O₃ (3.0 %), CaO (3.7 %) and MgO (1.1 %) relative to the amphibolites. Their contents in Na₂O (4.7 %) and K₂O (1.0 %) are also higher than those of amphibolites. LOI values are high (1.6 %). They have very high Sr (638 ppm) and Ba (665 ppm) contents; and moderate zirconium contents (101 ppm).

Baker et al. (1994) also demonstrated high contents in Al₂O₃ and SiO₂ with low contents in MgO and alkalis in monzogabbro accompanied by high Sr, Ba and Zr values. These high contents are most likely to retain the initial ratio of the mantle source region from which these magmas were derived. The extremely high Sr contents in the Monzogabbro may indicate the abundance of plagioclase phases in this rock (ukaegbu and ekwueme 2006). However, it is generally argued that low Mg# versus high SiO₂ rocks might not have interacted with the peridotitic mantle wedge, implying for instance their genesis in a flat subduction regime (e.g. Smithies et al. 2003), or an under plating tectonic setting that excluded the mantle wedge. Martin and Moyen (2002) also suggest that subducted slabs may have melted at a level shallow enough to have effectively precluded any interaction between the slab-melts and the mantle. Cerium, La and Nd are the most represented REE (Table 2). The REE patterns reveal enrichment of LREE and fractionation of HREE, positive cerium and slight negative europium anomalies (Fig. 4c). The enrichment of Nd along with Ce and La is interpreted as derived from a modified subcontinental lithosphere (Whalen et al. 2008).

Table 2: Trace Element Contents (In ppm) for Rocks of Akom II

Elements	Zingui				Kolasseng I												
	1		2		1			2			3			3			
	DL	Zn1	Zn2	GZn	AV1	AV2	NK1	NK2	NK3	NK4	NK5	NK7	FN3	AY1	AY2	AY3	NK6
Cr	3.00	591.00	558.00	34.00	389.00	285.00	81.00	199.00	278.00	234.00	96.00	222.00	174.00	199.00	198.00	203.0	11.00
V	0.80	239.3	205.20	39.30	283.70	293.2	334.70	261.60	285.20	260.50	338.60	273.7	347.40	307.20	290.20	309.40	113.30
Cu	1.40	134.10	3.90	25.60	243.20	214.30	105.80	398.20	203.80	295.90	204.60	356.20	178.60	362.50	290.10	107.30	10.20
Ni	1.60	218.60	158.40	15.70	184.30	143.50	66.70	133.50	143.20	129.00	89.10	143.00	130.50	131.80	142.20	133.50	11.20
Zn	7.00	63.00	206.00	41.00	108.00	97.00	126.00	236.00	91.00	94.00	97.00	129.00	99.00	113.00	107.00	107.00	45.00
Co	0.13	62.90	44.03	8.38	58.44	57.16	53.80	56.65	53.19	54.87	56.02	57.59	53.72	61.90	60.92	62.73	9.78
Sc	1.10	39.00	36.80	6.30	39.00	37.50	45.50	40.90	44.40	41.80	44.10	42.70	45.30	47.50	43.20	44.00	9.30
Ga	0.04	15.20	25.11	16.56	17.67	19.01	19.40	18.46	16.98	17.64	17.84	17.60	17.99	20.23	19.26	20.68	24.64
Zr	6.00	43.00	129.00	101.00	38.00	47.00	120.00	75.00	46.00	83.00	39.00	94.00	44.00	140.00	82.00	105.00	189.00
Y	0.05	17.21	69.14	8.17	22.19	27.30	39.40	36.63	20.25	39.41	25.52	34.12	25.30	47.36	29.63	28.22	10.00
Nb	0.03	2.26	14.68	3.62	3.38	3.92	6.68	4.86	3.26	5.06	3.35	4.66	3.25	5.95	4.17	5.13	4.20
Mo	0.08	0.19	0.16	0.16	0.34	0.38	0.57	0.64	0.35	0.98	1.12	0.38	0.33	0.52	0.34	0.44	<0.08
Sn	0.16	1.33	2.89	0.70	0.64	0.58	0.79	0.36	0.45	0.30	0.42	0.24	0.56	0.26	0.38	0.46	1.04
Tl	0.01	0.02	0.04	0.07	0.07	0.08	0.04	0.01	0.03	0.01	0.02	0.02	0.06	-	-	-	0.01
Cd	0.01	0.08	0.20	0.06	0.11	0.13	0.12	0.10	0.16	0.05	0.12	0.17	0.31	0.06	0.08	0.18	0.09
Sb	0.04	<0.04	0.05	0.04	<0.04	0.04	<0.04	<0.04	<0.04	0.31	<0.04	<0.04	0.04	<dl	<dl	<dl	<0.04
Cs	0.01	0.02	0.20	0.11	0.07	0.08	0.05	0.03	0.10	0.01	0.03	0.21	0.13	0.04	0.03	0.04	0.07
Hf	0.14	1.22	3.32	2.55	1.32	1.53	3.20	2.13	1.37	2.30	1.27	2.53	1.40	3.60	2.19	2.76	4.76
Pb	0.60	0.90	7.80	8.40	6.70	5.00	1.80	0.90	1.50	<0.60	1.50	1.50	11.10	0.80	2.60	2.10	7.80
Ta	0.02	0.14	0.46	0.18	0.23	0.26	0.46	0.32	0.22	0.32	0.23	0.30	0.23	0.41	0.26	0.32	0.14
W	0.05	<0.05	<0.05	<0.05	<0.05	<0.05	0.06	<0.05	0.06	0.05	<0.05	0.07	0.07	0.06	0.06	0.06	<0.05
Li	0.40	2.50	4.00	4.20	8.50	9.10	5.50	6.10	6.70	2.10	3.20	11.00	5.30	9.00	11.90	11.30	2.60
Rb	0.23	2.22	20.91	22.02	2.95	18.62	15.00	4.70	8.79	5.00	3.51	9.38	7.75	6.29	6.71	6.53	2.80
Sr	0.60	122.30	241.90	638.80	153.40	171.90	106.70	203.50	123.8	90.00	113.60	107.20	111.40	64.70	135.70	114.70	1008.60
Ba	0.80	59.70	178.00	665.60	143.10	107.70	173.70	47.50	44.40	55.50	35.00	10.40	47.30	66.40	80.70	84.00	47.20
Be	0.04	0.28	1.97	1.06	0.40	0.39	0.65	0.53	0.38	0.53	0.39	0.49	0.31	0.61	0.59	0.53	0.73
U	0.01	0.11	0.44	0.35	0.15	0.13	0.78	0.18	0.08	0.21	0.12	0.17	0.11	0.22	0.13	0.20	1.81
Th	0.02	0.37	9.60	1.96	0.46	0.45	3.11	0.73	0.28	0.61	0.45	0.66	0.34	0.80	0.52	0.69	11.75

d.l.: detection limit; LOI: Loss on Ignition 1: Amphibolites; 2: Monzogabbro; 3: Pyroxenite

Table 3: Rare Earth Element Contents (In ppm) for Rocks of Akom II

	Zingui				Kolasseng I												
	d.l.	1	2	1	1	2	3	3	3	3	3	3	3	3	3	3	3
		Zn1	Zn2	GZn	FN3	AV1	AV2	NK1	NK2	NK3	NK4	NK5	NK7	AY1	AY2	AY3	NK6
La	0.04	4.44	42.85	12.6	3.64	5.24	5.52	17.11	7.65	3.77	7.44	4.55	6.67	7.93	5.43	6.14	59.19
Ce	0.12	10.27	97.19	40.89	10.04	12.07	12.49	36.18	19.16	10.21	17.27	11.86	16.93	20.32	13.52	17.78	104.3
Pr	0.01	1.45	13.13	2.64	1.6	1.93	2.16	4.66	2.89	1.62	2.62	1.78	2.55	3.16	2.08	2.74	9.12
Nd	0.06	6.88	55.79	9.61	8.5	9.99	11.28	20.26	14.35	8.41	13.19	9.25	12.96	15.66	10.16	13.27	29.03
Sm	0.01	1.98	14.04	1.93	2.85	3.15	3.61	5.22	4.49	2.69	4.23	2.98	4.06	4.78	3.36	4.13	4.23
Eu	0.01	0.76	3.4	0.67	1.07	1.07	1.31	1.59	1.44	0.99	1.32	1.1	1.29	1.54	0.99	1.37	1.39
Gd	0.01	2.55	13.64	1.65	3.77	4.1	4.8	6.31	5.74	3.39	5.64	3.88	5.23	6.4	4.43	5.37	3.02
Tb	0.01	0.45	2.15	0.26	0.68	0.67	0.81	1.09	0.99	0.59	1.01	0.69	0.91	1.62	0.77	0.9	0.4
Dy	0.01	3.02	13.08	1.54	4.52	4.36	5.41	7.05	6.57	3.75	6.84	4.57	6.07	7.94	5.12	5.42	2.04
Ho	0.01	0.65	2.56	0.29	0.97	0.87	1.09	1.49	1.41	0.78	1.47	0.97	1.29	1.75	1.07	1.04	0.36
Er	0.01	1.93	7.16	0.84	2.82	2.39	3.05	4.22	4.08	2.26	4.35	2.87	3.83	5.44	3.2	2.8	0.92
Tm	0.01	0.28	0.99	0.12	0.42	0.33	0.41	0.63	0.59	0.32	0.62	0.41	0.54	0.8	4.47	0.38	0.12
Yb	0.01	1.84	6.1	0.77	2.73	2.04	2.5	4	3.84	2.03	3.98	2.7	3.54	5.1	3.03	2.27	0.73
Lu	0.01	0.28	0.85	0.11	0.41	0.29	0.36	0.59	0.56	0.3	0.57	0.4	0.52	0.77	0.45	0.33	0.11
ΣREE	-	36.78	272.9	73.92	44.02	48.5	54.8	110.4	73.76	41.11	70.55	48.01	66.39	83.21	54.09	63.93	214.96
LREE	-	25.78	226.4	68.34	27.7	33.45	36.37	85.02	49.98	27.69	46.07	31.52	44.46	53.38	35.54	45.43	207.26
HREE	-	11	46.53	5.58	16.32	15.05	18.43	25.38	23.78	13.42	24.48	16.49	21.93	29.82	18.54	18.51	7.7
A	-	2.34	4.87	12.25	1.7	2.22	1.97	3.35	2.1	2.06	1.88	1.91	2.03	1.79	1.92	2.45	26.92
(La/Yb) _N	-	1.42	4.14	9.65	0.79	1.51	1.3	2.52	1.17	1.1	1.1	0.99	1.11	1.06	1.22	1.84	45.39
Ce/Ce*	-	0.99	1.06		1.08	0.99	0.94	1.05	1.06	1.07	1.02	1.08	1.07	0.98	0.96	1.05	1.17
Eu/Eu*	-	1.03	0.75		0.99	0.2	0.96	0.84	0.86	0.99	0.82	0.99	0.85	0.85	0.78	0.89	1.19

d.l.: detection limit; LOI: Loss on Ignition 1: Amphibolites; 2: Monzogabbro; 3: Pyroxenite

A: LREE/HREE; dl: detection limits. 1: Amphibolites ; 2: Monzogabbro ; 3: Pyroxenite

$Ce/Ce^* = (Ce_{sample}/Ce_{chondrite}) / (La_{sample}/La_{chondrite})^{1/2} (Pr_{sample}/Pr_{chondrite})^{1/2}$

$Eu/Eu^* = (Eu_{sample}/Eu_{chondrite}) / (Sm_{sample}/Sm_{chondrite})^{1/2} (Gd_{sample}/Gd_{chondrite})^{1/2}$

$(La/Yb)_N = (La_{sample}/La_{chondrite}) / (Yb_{sample}/Yb_{chondrite})$

The pyroxenites are silico-aluminous rocks. The high Al₂O₃ alongside TiO₂ content of the rocks also suggest that the parental melt was a MORB type (Baumgartner et al. 2012). They show moderate Fe₂O₃ (5.5 %) and CaO (7.4 %) contents and low MgO contents. Na₂O

contents are also high relative to amphibolites and monzogabbro. Pyroxenite of Nyabitande have outstanding Sr (1009 ppm) contents, and moderate Zr (189 ppm) and V (113 ppm) contents. The rock is richer in LREE; it has high LREE/HREE ratios and high fractionation index. The high fractionation indices in pyroxenite is linked to a high rate of fractionation of REE confirming the depletion in HREE (Nédélec et al. 1990). The REE patterns reveal negative europium anomaly; an enrichment of LREE and depletion in HREE (Fig. 4c).

5. Discussion

5.1 Geochemical characteristics of amphibolites

The mineralogy of the garnet amphibolites of Akom II includes hornblende + plagioclase + garnet ± quartz ± epidote ± apatite ± opaque, this is consistent with that of garnet amphibolites from the metamorphic sole of the Muslim Bagh ophiolite (Pakistan; Kakar et al. 2015). The mineral assemblages of the garnet amphibolites rocks indicate that they could have been formed from the basic igneous protolith. The low CaO, Na₂O, K₂O and TiO₂ contents in amphibolite of Nyabitande are also consistent with those of the ultramafic rocks of Pindar (Balarum et al. 2013). These contents suggest a high degree of partial melting from the depleted mantle source, which prevailed during the development of the rocks.

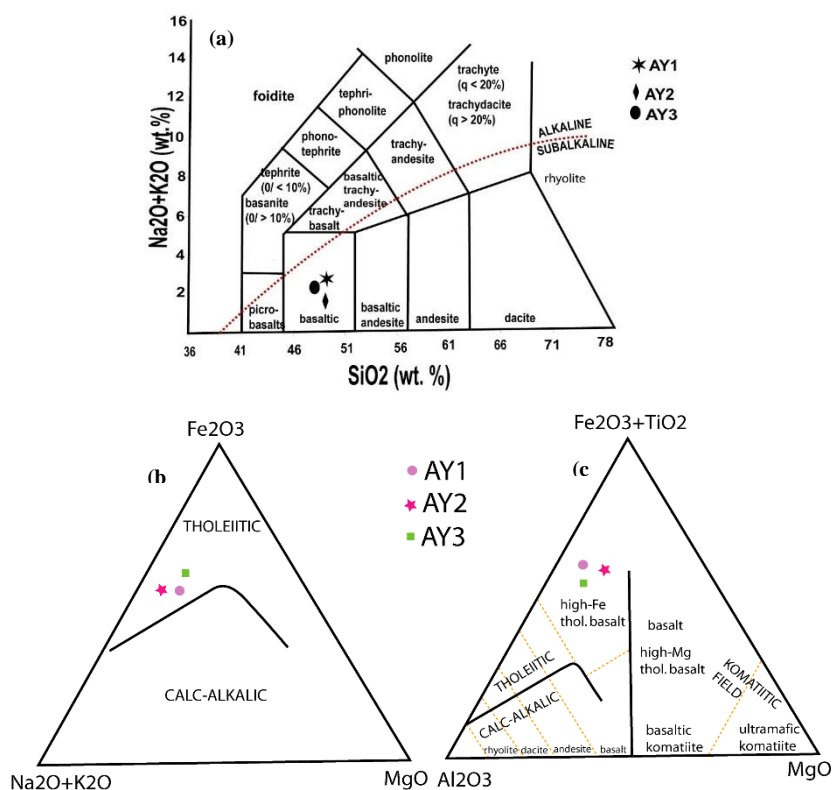


Fig. 5: Geotectonic Diagrams of Total Alkali and Silica (TAS) After Le Bas Et Al. (1986) and Jensen's Cation Plot (Jensen 1976).

The negative Eu anomaly associated with light rare earth elements (LREE) enrichment depicts the evolution of the rocks initially through fractional crystallization (V. Balarum et al. 2013). Leybourne et al. (2008) showed that the negative Eu anomalies are the result of an intense fractionation of REE. The high degree of fractionation of REE is confirmed by the depletion in HREE (Nedelec et al. 1990). Geochemically, it appears that the ortho-amphibolites of Nyabitande are derived from basalts with a depleted mantle source (Srivastava 2012). REE patterns also support this inference; the rocks show flat REE patterns. These patterns also suggest that melt responsible for these rocks may be generated through high-percentage (~20-25%) melting of a depleted mantle (Condie et al. 1997; Srivastava 2012). Rocks derived from such melt may show almost flat REE patterns ($(La/Yb)_N = 1.40 - 1.82$), the case of these rocks, with exceptions of few samples (Table 3).

5.2. Geotectonic context of amphibolites

Selected amphibolite samples (AY1, AY2 and AY3) from Nyabitande were chemically classified by major and trace elements using the total alkali and silica (TAS) (Le Bas et al. 1986). The TAS diagram aids in the determination of the geotectonic context of amphibolites (Fig. 5a). This diagram, show that the amphibolites of Nyabitande were derived from a basaltic protolith. According to the geotectonic diagram of Irvine and Baragar (1971), the basalt that is at the origin of these amphibolites is tholeiitic in nature (Fig. 5b). This view is consistent with that of Kakar et al. (2015).

Also the Jensen's cation plot (Jensen 1976) shows that the protolith is high-Fe tholeiitic basalt (Fig. 5c). The triangle of total rocks according to La Roche (1965) also confirms that the protolith of these amphibolites is not sedimentary but magmatic and very close to basalt in nature (Fig. 6). The overall low contents in several major and trace elements including REE confirm the basic nature of the rocks.

Given that the amphibolite of Akom II have undergone at least one metamorphic event, it can be expected that they should have suffered significant element mobility, especially involving the alkali and LIL elements (M.T. Gómez-Pugnaire et al. 2003). Therefore, the alkaline

character of some of the igneous protoliths should also be regarded with caution. A better classification can be attempted drawing on those elements less sensible to the metamorphic mobility, such as the high field strength elements (HFSE). The amphibolites of Akom II show low Nb/Y ratios (0.1 - 0.6). According to Floyd and Winchester, 1975; M.T. Gómez-Pugnaire et al. 2003, low Nb/Y ratios (<0.7) can be concluded to reveal a clear tholeiitic affinity in the samples studied. This is also confirmed by the geotectonic diagrams developed after Irvine and Baragar (1971; Fig. 5b and c).

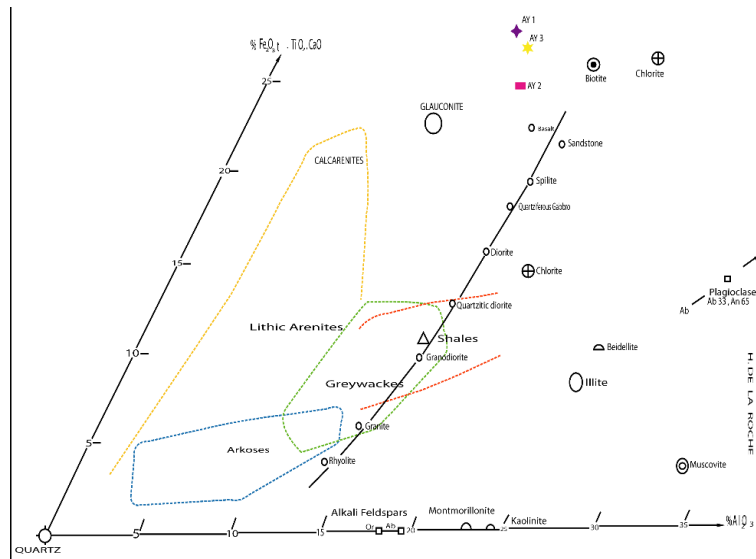


Fig. 6: The Triangle of Total Rocks According to La Roche (1965).

According to Xia (2014), the Zr concentration in arc basalts is usually below 130 ppm and below 3.3 Zr/Y ratio. In continental basalts, these values are above 70 ppm of Zr and above 3.4 Zr/Y (regardless of its contamination). Amphibolite samples of Akom II have between 38 and 129 ppm of Zr except for one sample (77 ppm in average) and 1.5 to 3.7 in Zr/Y ratio (2.3 in average; Table 2). These results also reveal arc basalts inclinations for the studied samples. Also, uncontaminated and contaminated continental basalts have similar Nb concentrations (7–49 ppm), but different Nb/La ratios (> 1.0 and < 1.0, respectively), while the modern arc basalt have low Nb (< 1.2 ppm) and Nb/La ratio (< 0.7). The analyzed samples in this paper have 2.26 to 6.68 ppm of Nb except for one sample (4.30 ppm in average) and 0.34 to 0.84 Nb/La ratio (0.68 in average), indicating intermediary results between an arc basalt and contaminated continental basalt (Bicalho et al. 2019). Primitive mantle-normalized (Sun and McDonough 1989) REE (Table 3) patterns reveal negative slight negative Nb, Ce, Ta and Ti for several samples (Fig. 7). According to Polat (2014), negative Nb and Ti anomalies are consistent with a juvenile ocean island arc origin, a metasomatic mantle wedge source for tholeiitic suite. Amphibolites of Akom II present Nb/Ta ratios (Fig. 8) that range from 14 – 16 (15.12 on average). According to Coira and Kay (1993), the Nb/Ta ratios ranging between 12.5 and 20 correspond to Volcanic Arc Basalt (VAB). The negative anomalies in Ta and Ti for some samples shown by the primitive mantle-normalized patterns (Fig. 7), suggest a geotectonic signature characteristic of a subduction zone, consequently suggesting the existence of a suture zone in the study area (Fotzing et al. 2019).

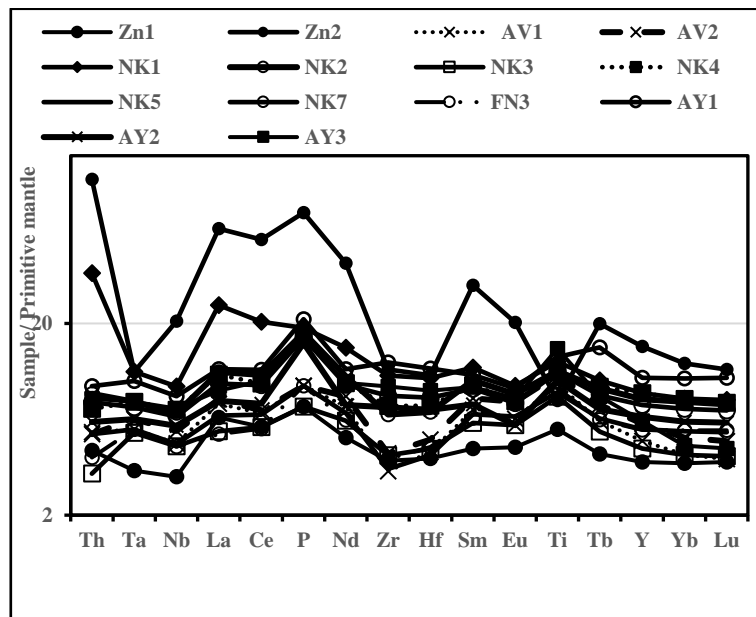


Fig. 7: Primitive Mantle Normalized Incompatible Trace Element Spider Diagram (After Sun & McDonough 1989).

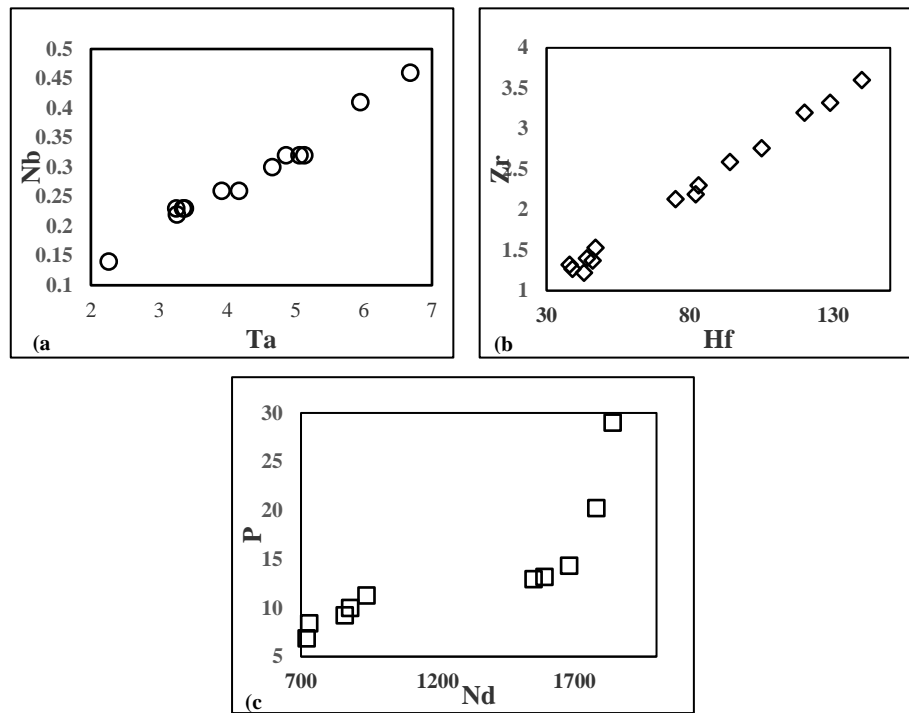


Fig. 8: Variation Diagrams A) Nb/Ta, B) Zr/Hf, and C) P/Nd.

6. Conclusions

The present study conclusively establishes the generation of amphibolites of the Akom II based on their mineral assemblages, geochemical affinities and geotectonic settings. From the above discussion the following conclusions are drawn:

- 1) The studied rocks of Akom II are garnet amphibolites. Mineralogically, the rocks contain hornblende + plagioclase + garnet \pm quartz \pm epidote \pm apatite \pm opaque. The mineral assemblages suggest that they are metamorphosed basaltic rocks.
- 2) The geochemical signature indicates that the amphibolites of Akom II are tholeiitic in nature. They are similar to the metamorphosed equivalents of ocean island basalts (OIB), with characteristics typical of Volcanic Arc-Basalt (VAB).
- 3) The geotectonic diagrams, high field strength elements ratios (HFSE) and rock/chondrite patterns confirm the nature and tectonic setting of these rocks and also indicate a past subduction zone in the area.

Acknowledgements

We are grateful to the team at GeoLabs (Sudbury, Canada), for partly financing the whole rock analyses including sample preparation and laboratory analyses. We also appreciate the members of the Department of Applied Geosciences of the University of Leoben (Austria) for thin section observations under metallographic microscope.

References

- [1] Aye BA, Sababa E & Ndjigui PD (2017), Geochemistry of S, Cu, Ni, Cr and Au-PG from in the garnet amphibolites the Akom II area in the Archaean Cameroon. *Chemie der Erde* 77, 81–93. <https://doi.org/10.1016/j.chemer.2017.01.009>.
- [2] Baker IA, Gamble JA & Graham IJ (1994), The age, geology and geochemistry of the Tapuaenuku Igneous Complex, Marlborough, New Zealand. *Journal of Geology and Geophysics* 37:3, 249-268. <https://doi.org/10.1080/00288306.1994.9514620>.
- [3] Balam V, Singh SP, Satyanarayanan M & Anjaiah KV (2013), Platinum group elements geochemistry of ultramafic and associated rocks from Pindar in Madawara Igneous Complex, Bundelkhand massif, central India. *Journal of Earth Systems Sciences* 122, 1, 79–91. <https://doi.org/10.1007/s12040-012-0260-0>.
- [4] Baumgartner RJ, Zaccarini F, Garuti G & Thalhhammer, OAR (2012), Mineralogical and geochemical investigation of layered chromitites from the Bracco–Gabbro complex, Ligurian ophiolite, Italy. *Contributions to Mineralogy and Petrology* 165, 477– 493. <https://doi.org/10.1007/s00410-012-0818-5>.
- [5] Condie KC (1997), Sources of proterozoic mafic dyke Swarms: constraints from Th/Ta and La/Yb ratios. *Precambrian Research* 81, 3–14. [https://doi.org/10.1016/S0301-9268\(96\)00020-4](https://doi.org/10.1016/S0301-9268(96)00020-4).
- [6] De La Roche H (1965), Sur l'existence de plusieurs faciès géochimiques dans les schistes paléozoïques des pyrénées luchonnaises. *Geologische Rundschau* 55, 274–301. <https://doi.org/10.1007/BF01765767>.
- [7] Ebah Abeng SA, Ndjigui P-D, Aye AB, Tessontsap T & Bilong P (2012), Geochemistry of pyroxenites, amphibolites and their weathered products in the Nyong unit, SW Cameroon (NW border of Congo craton): implications for Au-PGE exploration. *Journal of Geochemical Exploration* 114, 1-19. <https://doi.org/10.1016/j.gexplo.2011.11.003>.
- [8] Faleiros FM, Ferrari VC, Costa VS & Campanha GAC (2011), Geoquímica e petrogênese de metabasitos do Grupo Votuverava (Terreno Apiaí, Cinturão Ribeira Meridional): Evidências de uma bacia retroarco Calimiana. *Geologia USP, Série Científica* 11(2):135-155. <https://doi.org/10.5327/Z1519-874X2011000200008>.
- [9] Floyd PA & Winchester JA (1975), Magma-type and tectonic setting discrimination using immobile elements. *Earth Planetary Science Letters* 27, 211–218. [https://doi.org/10.1016/0012-821X\(75\)90031-X](https://doi.org/10.1016/0012-821X(75)90031-X).
- [10] Fozing EM, Kwékam M, Dedzo MG, Asaah NE A, Njanko T, Kouémo JT, Awoum JE & Njonfang E (2019), Petrography and geochemistry of amphibolites from the Fomopéa Pluton (West Cameroon): Origin and geodynamic setting. *Journal of African Earth Sciences* 154, 181–194. <https://doi.org/10.1016/j.jafrearsci.2019.03.024>.

- [11] Gomez-Pugnaire MT, Azor A, Fernandez-Soler J M & Lopez Sanchez-Vizcaino V (2003), The amphibolites from the Ossa–Morena / Central Iberian Variscan suture (Southwestern Iberian Massif): geochemistry and tectonic interpretation. *Lithos* 68, 23–42. [https://doi.org/10.1016/S0024-4937\(03\)00018-5](https://doi.org/10.1016/S0024-4937(03)00018-5).
- [12] Jensen LS (1976), A new cation plot for classifying subalkalic volcanic rocks. *Ontario Geological Survey Miscellaneous paper* 66.
- [13] Irvine TN, & Baragar W.R.A (1971), A guide to the chemical classification of the common volcanic rocks. *Canadian Journal of Earth Sciences* 8, 523-548. <https://doi.org/10.1139/e71-055>.
- [14] Kakar M I, Khan M, Mahmood K, & Kerr A C (2014), Facies and distribution of metamorphic rocks beneath the Muslim Bagh ophiolite (NW Pakistan): tectonic implications. *Journal of Himalayan Earth Sciences*. 47 (2).
- [15] Kakar MI, Mahmood K, Khan & Plavska D (2015), Petrology and geochemistry of amphibolites and greenschists from the metamorphic sole of the Muslim Bagh ophiolite (Pakistan): implications for protolith and ophiolite emplacement. *Arabian Journal of Geosciences* 8, 6105–6120. <https://doi.org/10.1007/s12517-014-1613-6>.
- [16] Le Bas MJ, Le Maitre RW, Streckeisen A & Zanettin B (1986), A chemical classification of volcanic rocks based on total alkali-silica diagram. *Journal of Petrology* 27, 745-750. <https://doi.org/10.1093/petrology/27.3.745>.
- [17] Leybourne M I & Johannesson K H (2008), Rare earth elements (REE) and yttrium in stream waters, stream sediments, and Fe–Mn oxyhydroxides: fractionation, speciation, and controls over REE+Y patterns in the surface environment. *Geochimica et Cosmochimica Acta* 72, 5962–5983. <https://doi.org/10.1016/j.gca.2008.09.022>.
- [18] Maniesi V & Oliveira MAF (2000), Petrogênese dos metabasitos com afinidades dos toleítos de fundo oceânico das regiões de Adrianópolis Campo Largo / PR. *Revista Brasileira de Geociências* 30 (4), 607-614. <https://doi.org/10.25249/0375-7536.2000304607614>.
- [19] Martin H & Moyen J-P, (2002), Secular changes in tonalite–trondhjemite–granodiorite composition as markers of the progressive cooling of Earth. *Geology* 30, 319–322. [https://doi.org/10.1130/0091-7613\(2002\)030<0319:SCITG>2.0.CO;2](https://doi.org/10.1130/0091-7613(2002)030<0319:SCITG>2.0.CO;2).
- [20] Maurizot P, Abessolo A, Feybesse A, Johan J.L & Lecomte P (1986) Etude et prospection minières du Sud-Ouest Cameroun. *Synthèse des travaux de 1978 à 1985. 85-CMR 066. BRGM*.
- [21] McDonough WF & Sun S-S (1995), The composition of the Earth. *Chemical Geology* 120, 223-253. [https://doi.org/10.1016/0009-2541\(94\)00140-4](https://doi.org/10.1016/0009-2541(94)00140-4).
- [22] Mountain BW & Wood SA (1988), Chemical controls on the solubility, transport, and deposition of platinum and palladium in hydrothermal solutions: a thermodynamic approach. *Economic Geology* 83, 492-510. <https://doi.org/10.2113/gsecongeo.83.3.492>.
- [23] Munyanyiwa H (1997), Geochemistry of amphibolites and quartzofeldspathic gneisses in the Pan-African Zambezi belt, northwest Zimbabwe: evidence for bimodal magmatism in a Continental rift setting. *Precambrian Research* 81, 179-196. [https://doi.org/10.1016/S0301-9268\(96\)00034-4](https://doi.org/10.1016/S0301-9268(96)00034-4).
- [24] Nédélec A, Nsifa EN & Martin H (1990), Major and trace element geochemistry of the Archaean Ntem plutonic complex (South Cameroon): petrogenesis and crustal evolution. *Precambrian Research* 47, 35–50. [https://doi.org/10.1016/0301-9268\(90\)90029-P](https://doi.org/10.1016/0301-9268(90)90029-P).
- [25] Nzenti JP, Barbey P, Macaudiere JP & Soba D (1988), Origin and evolution of the late Precambrian high grade Yaoundé gneisses (Cameroon). *Precambrian Research* 38, 91–109. [https://doi.org/10.1016/0301-9268\(88\)90086-1](https://doi.org/10.1016/0301-9268(88)90086-1).
- [26] Polat A (2014), Geochemistry of subduction-related mafic to felsic volcanic rocks of the late Archean Wawa greenstone belts, Superior Province, Canada. *Journal of Geophysics and Engineering Science* 51, 277–295. <https://doi.org/10.1007/s007770050064>.
- [27] Penaye J, Toteu SF, Michard A, Bertrand JM & Dautel D (1989), Reliques granulitiques d'âge Protérozoïque inférieur dans la zone mobile Panafricaine d'Afrique Centrale au Cameroun: géochronologie U/Pb sur zircons. *Comptes rendus de l'Académie des Sciences Paris* 309, 315–318.
- [28] Penaye J, Toteu SF, Tchameni R, Van Schmus W R, Tchakounté J, Ganwa A, Minyem D & Nsifa, NE (2004), The 2.1 Ga West African Belt in Cameroon: extension and evolution. *Journal of African Earth Sciences* 39, 1196-1202. <https://doi.org/10.1016/j.jafrearsci.2004.07.053>.
- [29] Shang CK, Liégeois J-P, Satir M & Nsifa EN (2010), Late Archaean high-K granite geochronology of the northern metacratonic margin of the Archaean Congo craton. Southern Cameroon: evidence for Pb-loss due to non-metamorphic causes. *Gondwana Research* 18, 337-355. <https://doi.org/10.1016/j.gr.2010.02.008>.
- [30] Smithies RH, Champion DC & Cassidy KF (2003), Formation of Earth's early Archaean continental crust. *Precambrian Research* 127, 89–101. [https://doi.org/10.1016/S0301-9268\(03\)00182-7](https://doi.org/10.1016/S0301-9268(03)00182-7).
- [31] Srivastava RK (2012), Petrological and Geochemical Studies of Paleoproterozoic Mafic Dykes from the Chitrangi Region, Mahakoshal Supracrustal Belt, Central Indian Tectonic Zone: Petrogenetic and Tectonic Significance. *Journal Geological Society of India* 80, 369-381. <https://doi.org/10.1007/s12594-012-0155-3>.
- [32] Sun SS & McDonough WF (1989), Chemical and Isotopic Systematic of Oceanic Basalts: Implication for Mantle Composition and Processes. In: Saunder, A.D. and Norry, M.J., Eds., *Magmatism in the Ocean Basins, Geological Society, Special Publications London* 42, 313-345. <https://doi.org/10.1144/GSL.SP.1989.042.01.19>.
- [33] Szczepanski J & Oberc-Dziedzic T (1998), Geochemistry of amphibolites from the Strzelin crystalline massif, Fore-Sudetic Block, SW Poland. *Journal of Mineralogy and Geochemistry* 173, 23 – 40. <https://doi.org/10.1127/njma/173/1998/23>.
- [34] Tchameni R, Pouclot A, Mezger K, Nsifa EN & Vicat JP (2004), Single zircon Pb-Pb and Sm-Nd whole rock ages for the Ebolowa greenstone belts: evidence for pre-2.9 Ga terranes in the Ntem Complex (South Cameroon). *Journal of Cameroon Academic Sciences* 4, 235-246.
- [35] Toteu SF, Van Schmus WR, Penaye J & Nyobe JB (1994), U-Pb and Sm-Nd evidence for Eburmean and Pan-African high-grade metamorphism in cratonic rocks of southern Cameroon. *Precambrian Research* 67, 321-347. [https://doi.org/10.1016/0301-9268\(94\)90014-0](https://doi.org/10.1016/0301-9268(94)90014-0).
- [36] Toteu SF, Yongue RF, Penaye J, Tchakounte J, Seme Mouangue AC, Van Schmus WR, Deloule E & Stendal H (2006), U–Pb dating of plutonic rocks involved in the nappe tectonic in southern Cameroon: consequence for the Pan-African orogenic evolution of the central African fold belt. *Journal of African Earth Sciences* 44, 479–493. <https://doi.org/10.1016/j.jafrearsci.2005.11.015>.
- [37] Xia LQ 2014, The geochemical criteria to distinguish continental basalts from arc related ones. *Earth-Science Reviews* 139, 195-212. <https://doi.org/10.1016/j.earscirev.2014.09.006>.
- [38] Xu D, Xia B, Bakun-Czubarow N, Bachlinski R, Li P, Chen G & Chen T (2008) Geochemistry and Sr-Nd isotope systematic of metabasites in the Tunchang area, Hainan Island, South China: implications for petrogenesis and tectonic setting. *Mineralogy and Petrology* 92 (3-4), 361-391. <https://doi.org/10.1007/s00710-007-0198-0>.
- [39] Wang YC, Prichard HM, Zhou MF & Fisher PC (2008) Platinum-group minerals from the Jinbaoshan Pd-Pt deposit, SW China: evidence for magmatic origin and hydrothermal alteration. *Mineralium Deposita* 41, 791-803. <https://doi.org/10.1007/s00126-008-0196-0>.